THE JOURNAL OF COMPARATIVE NEUROLOGY 497:416–435 (2006)

Thalamocortical Connections of Anterior and Posterior Parietal Cortical Areas in New World Titi Monkeys

JEFFREY PADBERG AND LEAH KRUBITZER*
Center for Neuroscience and Department of Psychology, University of California–Davis, Davis, California 95616

ABSTRACT

We examined the thalamocortical connections of electrophysiologically identified locations in the hand and forelimb representations in areas 3b, 1, and 5 in the New World titi monkeys (*Callicebus moloch*), and of area 7b/AIP. Labeled cells and terminals in the thalamus resulting from the injections were related to architectonic boundaries. As in previous studies in primates, the hand representation of area 3b has dense, restricted projections predominantly from the lateral division of the ventral posterior nucleus (VPl). Projections to area 1 were highly convergent from several thalamic nuclei including the ventral lateral nucleus (VL), anterior pulvinar (PA), VPl, and the superior division of the ventral posterior nucleus (VPs). In cortex immediately caudal to area 1, what we term area 5, thalamocortical connections were also highly convergent and predominantly from nuclei of the thalamus associated with motor, visual, or somatic processing such as VL, the medial pulvinar (PM), and PA, respectively; with moderate projections from VP, central lateral nucleus (CL), lateral posterior nucleus (LP), and VPs. Finally, thalamocortical connections of area 7b/AIP were from a range of nuclei including PA, PM, LP/LD, VL, CL, PL, and CM. The current data support two conclusions drawn from previous studies in titi monkeys and other primates. First, cortex caudal to area 1 in New World monkeys is more like area 5 than area 2. Second, the presence of thalamic input to area 5 from both motor nuclei and somatosensory nuclei of the thalamus, suggests that area 5 could be considered a highly specialized sensorimotor area. J. Comp. Neurol. 497:416–435, 2006.

Indexing terms: primary somatosensory area; area 1; area 5; AIP; ventral posterior nucleus; ventrolateral nucleus; area 7b

Posterior parietal cortex is a relatively large region of cortex that resides between somatosensory cortical fields located rostrally, and visual fields located caudally, and contains a number of complexly organized cortical fields such as areas 5, LIP, VIP, AIP, and PRR, to name a few (see abbreviations list). Elegant studies in awake behaving monkeys have demonstrated that these cortical areas are very different from the pure sensory cortical fields from which they ultimately receive their inputs, and these areas are thought to be involved in generating body-centered and eye-centered coordinate reference frames which are necessary for reaching and grasping objects in immediate extrapersonal space (Andersen and Buneo, 2002; Ferraina and Bianchi, 1994; Kalaska, 1996; Kalaska et al., 1997; Lacquaniti et al., 1995; Wise et al., 1997). From a cognitive perspective, these fields are involved in generating what would be considered a "sense of self" or an internal representation of the body (e.g., Dubowitz et al., 1998; Fogassi et al., 2005; Iriki et al., 2001; see Krubitzer and Disbrow, 2006; Rizzolatti et al., 2001 for review). This would include a tacit knowledge of the state of joint articulation and muscle stretch of a body part, such as the hand, relative to the configuration of other body parts, such as the wrist, shoulder, and other hand. This also requires the animal to distinguish self-generated movements including head, eye, and hand movements,

Grant sponsor: NINDS; Grant number: RO1 NS35103-07; Grant sponsor: McDonnell (to L.K.); Grant sponsor: NEI (to J.P.); Grant number: F32 EY014503-01A1.

*Correspondence to: Leah Krubitzer, Center for Neuroscience, 1544 Newton Ct., Davis, CA 95616. E-mail: lakrubitzer@ucdavis.edu

Received 9 August 2005; Revised 4 November 2005; Accepted 23 February 2006

DOI 10.1002/cne.21005

Published online in Wiley InterScience (www.interscience.wiley.com).

and articulated sounds, from external stimuli and movements. Although the functional aspects of these behaviors are beginning to be revealed using modern imaging techniques (e.g., Disbrow et al., 1999; Dubowitz et al., 1998; Friedman et al., 2004; Logothetis et al., 1999; Shoham and Grinvald, 2001) and, as noted above, awake behaving monkey preparations, the anatomical substrate that ultimately generates this complex phenomenon is not well understood.

There are two lines of recent evidence that support the notion that posterior parietal areas should be considered as highly specialized sensorimotor areas derived for hand use in primates. The first line of evidence comes from studies of posterior parietal cortex in primates in which microstimulation of some of these areas induces highly complex, species-specific behaviors. For example, recent work by Cooke et al. (2003) on macaque monkeys in which the ventral intraparietal area was microstimulated demonstrated that defensive movements, including facial grimacing, eye closure, and hand to face movements, could be evoked. Likewise, microstimulation of rostral regions of posterior parietal cortex in galagos (Stepniewska et al., 2005), including area 5, evoked what the authors term "ethologically significant behaviors." In addition to defensive movements, these behaviors included reaching, hand to mouth, and aggressive behaviors.

The second line of evidence comes from studies that demonstrate that some posterior parietal areas, including area 5, are more densely connected with motor cortical fields than with somatosensory or visual cortical fields (e.g., Cavada and Goldman-Rakic, 1989; Lewis and Van Essen, 2000; Padberg et al., 2005; reviewed by Rizzolatti and Fadiga, 1998; Tanne-Gariepy et al., 2002). It is apparent from the studies described above that posterior parietal areas could be considered specialized motor integrators that allow the internal or animal-centered state to interface and explore the external animate and inanimate world. One objective of the present investigation is to determine which thalamic nuclei project to areas 5 and 7b/AIP, and may therefore contribute to these complex behaviors. A second, related objective is to determine whether, similar to the neocortex, thalamocortical connections of area 5 and 7b/AIP are strongly associated with motor processing.

The final objective of the present investigation is to determine the thalamocortical connections of anterior parietal cortical fields, and to identify the differences that we believe exist in New World and Old World monkeys. In a previous study of cortical connections of area 5, we proposed that area 5 is involved in the generation of an internal coordinate system described above, and that such a system is critical for all mammals, not just primates. What differs among species is how posterior parietal cortex is organized. The organization of posterior parietal cortex is dependent on the specialized peripheral morphology or "effector" of the animal, and the unique motor programs that allow each animal to interface their specialized effector with the objects in extra personal space to be explored (Krubitzer and Disbrow, 2006; Padberg et al., 2005).

For example, in primates, posterior parietal areas are dominated by the representation of the hand and are involved in generating motor sequences associated with the movement of the hands in extra personal space. This is different than the organization of a rodent, which is highly dependent on its vibrissae, or a star-nosed mole, which relies upon its nose rays. In this previous study, we further suggested that these differences manifest at very early stages of processing, and that the evolution of the opposable thumb may have led to dramatic changes in organization of anterior parietal areas. Such changes include the addition of an area 2, which provides input to

Abbreviations

Cortical areas and regions	
AIP	anterior intraparietal area
IPS	intraparietal sulcus
LIP	lateral intraparietal area
LS	lateral sulcus
M1	primary motor area
PM	premotor area
PRR	parietal reach region
S1	primary somatosensory area
V4	fourth visual area
VIP	ventral intraparietal area
Thalamic nuclei and subdivisions	
AD	anterior dorsal nucleus
AV	anterior ventral nucleus
CL	central lateral nucleus
CM	centromedial nucleus
Fr	fasciculus retroflexus
H	habenula
LD	lateral dorsal nucleus
LG	lateral geniculate nucleus
Lim	limitans nucleus
LP	lateral posterior nucleus
MD	mediodorsal nucleus
MG	medial geniculate nucleus
PA	anterior pulvinar nucleus
PC	paracentral nucleus
Pf	parafascicular nucleus
Pg	periacqueductal grey matter
PL	lateral pulvinar nucleus
PM	medial pulvinar nucleus
PO	posterior nuclear group
R	reticular nucleus
SC	superior colliculus
VA	ventroanterior nucleus
VIM	ventral intermediate nucleus
VL	ventrolateral nucleus
VP	ventroposterior nucleus or complex
VPi	ventroposterior nucleus, inferior
VPl	ventroposterior nucleus, lateral
VPm	ventroposterior nucleus, medial
VPs	ventroposterior nucleus, superior
ZI	zona inserta
Body parts	
d1–d5	digit 1 through digit 5
d	dorsal
dig	digit
el	elbow
fl	forelimb
glab	glabrous
ha	hand
he	head
wr	wrist
Tracers	
BDA	biotinylated dextran amine
FE	fluoroemerald
FR	fluororuby
HRP	horseradish peroxidase

TABLE 1. Tracers Injected

Case no.	Site	Representation	Amount/Tracer
01–79	Area 1	Distal forelimb	0.5 μl FR
	Area 5	Hand	0.4 μl FE
02–12	Area 1	Dorsal hand	0.3 μl FR
	Area AIP	–	0.3 μl BDA
02–18	Area 1	Dorsal hand	0.4 μl FR
	Area 5	Dorsal hand	0.4 μl FE
	Area AIP	–	0.4 μl BDA
02–52	Area 3b	d2 nailbed	0.4 μl BDA
	Area 1	Hand, forelimb	0.3 μl FR
	Area 5	Hand, digits	0.3 μl FE

posterior parietal fields, such as area 5 (e.g., Pearson and Powell, 1985; Pons and Kaas, 1986). Specifically, based on an examination of previous electrophysiological recording results and anatomical connectivity in a variety of New World monkeys and the prosimian galago, we proposed in our previous study that New World monkeys do not possess an area 2. Thus, our final objective for the present study is to examine the thalamocortical connections of area 1 and cortex caudal to area 1, which we term area 5, to determine whether connections of this region are more like those of area 2 or area 5 in Old World monkeys.

In these investigations we examined the thalamocortical connections of electrophysiologically defined locations in areas 3b, 1, and 5 by injecting anatomical tracers into electrophysiologically defined sites. Retrogradely labeled cells and terminal fields in the thalamus were related to architectonic distinctions. This allowed us to determine not only the global patterns of thalamocortical connections of a field, but to investigate the projections from specific nuclei of the thalamus to specific representations in the neocortex, such as the hand and forelimb representation in areas 3b, 1, and 5.

MATERIALS AND METHODS

Neuroanatomical tracing studies were combined with architectonic analysis in four titi monkeys (*Callicebus moloch*) to determine the thalamocortical connections of the hand and forelimb representations in areas 3b, 1, 5, and 7b/AIP. These animals were used in a previous study in which corticocortical connections were described (Padberg et al., 2005). In each case, electrophysiological mapping was performed to identify the stimulus preference and receptive fields in and around the injection site. All experimental protocols were approved by the Animal Use and Care Administrative Advisory Committee of the University of California, Davis and conformed to National Institutes of Health guidelines.

Injections of anatomical tracers

Ten injections of anatomical tracers were made in four animals (Table 1). Animals were initially anesthetized with either telazol (10 mg/kg) or ketamine hydrochloride (10 mg/kg), and then intubated and cannulated. Surgical levels of anesthesia were maintained with the inhalation anesthetic, isoflurane (1–3%). The animals were artificially ventilated throughout the experiment. A continuous infusion of lactated Ringer solution (6 ml/kg/hour) was given intravenously, and throughout the experiment the animal's heart rate, respiration rate, temperature, and expired pCO_2 levels were monitored and maintained. Once anesthetized and stabilized, the skin was cut, the temporalis muscle was retracted, and a craniotomy was made over the posterior parietal cortex. The dura was cut and the dura flaps were gently pulled away from the opening. The intraparietal sulcus (IPS) and lateral sulcus (LS) were visualized, and the location of the hand representations in areas 3b, 1, area 5, and 7b/AIP were approximated from previous maps made in titi monkeys. Excluding those placed in 7b/AIP, all injection sites were later verified using electrophysiological recording techniques (see below). Injections were made with a calibrated Hamilton syringe that was lowered into the cortex using a stereotaxically guided micromanipulator (Kopf Instruments, Tujunga, CA). Injections of 0.3–0.5 μl of the fluorescent tracers Fluoro-emerald (7% FE; Molecular Probes, Eugene, OR), Fluoro-ruby (FR, 7%; Molecular Probes), or biotinylated dextran amine (BDA; 10%) were made into areas 3b, 1, 5, and 7b/AIP in the left hemisphere (see Table 1). After the injections were complete, the brain was covered with a sterile contact lens, the dura flaps were placed over the lens, gel foam was placed over the dura flaps, and either the skull was replaced and held in place with acrylic, or a new skull was made from acrylic. The temporal muscle was sutured in place, and the skin was sutured. A recovery period of 6–12 days followed, to allow for transport of the neuroanatomical tracers before beginning acute electrophysiological recordings. Standard sterile surgical procedures were used throughout these surgeries.

Electrophysiological recordings were obtained with low-impedance tungsten-in-varnish microelectrodes (5 MΩ at 100 Hz), and the neural response was amplified, filtered, and monitored through a loud speaker and an oscilloscope. The electrode was placed perpendicular to the cortical surface, and a stepping hydraulic microdrive (Kopf Instruments) was used to lower the electrode in increments of 500 μm into the cortex. Once the electrode was in place, the body surface was stimulated, and the receptive fields for neurons at that site were drawn on diagrams of the monkey's body. Cutaneous stimulation consisted of light displacement of skin and hair with a fine probe, small puffs of air, and light brushing. Light to moderate taps, limb manipulation, and pressure were used to stimulate deep receptors of the muscles, joints, and skin. Visual stimulation consisted of full-field flashes of light, bars of light, and spots of light moved across the contralateral visual hemifield or flickered within the contralateral visual hemifield. Auditory stimulation consisted of clicks. In all animals, somatosensory, visual, and auditory stimulation was used, and the contralateral and ipsilateral body surface, joints, and musculature were stimulated. In all animals that received injections of anatomical tracers in areas 3b, 1, or 5, the injection site was electrophysiologically identified before perfusion by recording from cortex at, and immediately surrounding, the center of the injection site (see Padberg et al., 2005 for details).

Histology

Upon completion of the electrophysiological mapping session, each animal was transcardially perfused with 0.9% saline, followed by 4% paraformaldehyde in phosphate buffer (pH = 7.2–7.4), and 4% paraformaldehyde with 10% sucrose phosphate buffer. The brain was removed from the skull, and each hemisphere was carefully removed from the underlying thalamus and brainstem. The thalamus and flattened neocortex were placed into

phosphate buffer with 30% sucrose and left to soak overnight in this solution.

In all cases, the thalamus was sectioned coronally at a thickness of 50 μm on a freezing microtome, and series of sections were processed for CO histochemistry. In three cases, Nissl staining was also performed. With both techniques, most subdivisions of the thalamus were readily observed. Alternate series of sections were processed for fluorescence microscopy, and BDA (Veenman et al., 1992). Processing for BDA was done using standard ABC methods (Vectastain Elite; Vector Laboratories, Burlingame, CA).

Data analysis

Data analysis was performed in two separate stages. First, the series of sections that were mounted for fluorescent microscopy or processed for BDA were analyzed using a computerized X/Y stage encoding system (Accustage, Inc., Shoreview, MN). For the series of sections in each case, labeled cells and terminals were plotted along with tissue artifacts, blood vessels, and section outlines. The second stage of our analysis consisted of drawing architectonic boundaries from the entire series of sections processed for CO histochemistry and/or Nissl substance using a camera lucida. These drawings also included the outline of the section, blood vessels, and tissue artifacts.

The reconstructed tracer data were then aligned with the reconstructed architectonic data, using blood vessels, tissue artifacts, and tissue outlines, to determine the locations within the thalamus containing labeled cells, terminals, and axons. Finally, photomicrographs and drawings of the reconstructed data were generated and assembled using Canvas (ACD Systems, Saanichton, B.C.) and Adobe Photoshop (Adobe Systems, Inc.; San Jose, CA) software. Minor adjustments to brightness and contrast of the photomicrographs were made in Photoshop using adjustment layers.

For a full description of how cortical fields were subdivided using electrophysiology combined with architectonic analysis, and how injection sites were related to these cortical areas and body part representations within these fields, see Padberg et al. (2005).

RESULTS

In the following results, we examine the thalamocortical connections of cortical areas 3b, 1, 5, and 7b/AIP. We first describe the subdivisions of the dorsal thalamus in the titi monkey using CO and Nissl stains. We then describe the patterns of label in the different nuclei in the thalamus that resulted from injections into different electrophysiologically defined subdivisions in the neocortex.

Architectonic subdivisions of the thalamus

In describing thalamic nuclei in the current study of titi monkey thalamus, we use most of the divisions and nomenclature described in a recent study in titi monkeys in which thalamocortical connections of some somatosensory cortical fields were described (Coq et al., 2004), and of studies in other New World monkeys and Old World monkeys (Disbrow et al., 2002; Emmers and Akert, 1963; Huffman and Krubitzer, 2001; Jones, 1985; Krubitzer and Kaas, 1992; Stepniewska et al., 1994a).

Rostrally, the anteroventral nucleus (AV) reacted darkly for CO and contained small darkly stained cells in tissue stained for Nissl substance (Fig. 1A, B). The ventral anterior nucleus (VA) was located ventral and lateral to AV, reacted moderately for CO (Fig. 1A, C), and contained darkly stained, medium to large neurons with moderate packing density (Fig. 1B, D). The ventrolateral nucleus (VL) was located ventral and lateral to VA and dorsal to the ventroposterior complex. The VL reacted moderately for CO, and medium to large, moderate to densely packed neurons were observed in the Nissl staining (Fig. 1C, E; D, F). The boundary between VL and VA was sometimes difficult to distinguish.

The lateral and medial divisions of the ventral posterior nucleus (VPl and VPm) were readily distinguished with both CO (Fig. 1E, G, I) and Nissl stains (Fig. 1F, H, J). Both VPm and VPl stained darkly for CO and contained large, darkly stained neurons that were densely packed. Although VPm and VPl were similar in appearance, each division was separated by a lightly stained (CO) and cell sparse septa (Fig. 1G, H). Furthermore, VPl was more fragmented than VPm and separated by several small interleaving septa (Fig. 1G, H). In all cases, the inferior division of VP (VPi) was stained lightly for CO and contained very small, lightly stained cells that were very loosely packed. VPi has been proposed to possess finger-like extensions that form the septa in VPl and VPm (see Krubitzer and Kaas, 1992; Fig. 1E, G). The superior division of VP (VPs) was moderately stained for both CO and Nissl (Fig. 1G, H).

Ventral and slightly medial to AV, the centrolateral nucleus (CL) reacted darkly for CO, but was less homogeneous than AV (Fig. 1A, C, E). The CL was also darkly stained for Nissl, with moderately dense, large cells (Fig. 1B, D, F). Near the caudal portion of CL, the centromedian nucleus (CM) stained lightly for CO (Fig. 1G, I) and contained moderately packed, small- to medium-sized, darkly stained neurons (Fig. 1H, J). In both the CO and Nissl series, the dorsal, lateral, and ventral borders of CM were clearly marked by the internal medullary lamina (Fig. 1G–J).

The mediodorsal nucleus (MD) was located dorsal to CM, and medial to CL, and was moderately reactive for CO and appeared relatively homogeneous (Fig. 1A, C, E, G, I). In the Nissl series, MD was not homogeneous in appearance, but the large body of the nucleus contained medium to large, darkly stained cells, which were densely packed (Fig. 1B, D, F, H, J). In Nissl preparations, especially more caudally, the ventrolateral border of MD was clearly defined by the internal medullary lamina (Fig. 1H, J).

The laterodorsal nucleus (LD) and lateroposterior nucleus (LP) were located along the dorsal edge of the thalamus, and were observed to react moderately to intensely for CO (Fig. 1E, G, I). In the Nissl series, both LD and LP were observed to contain small darkly stained cells that were moderately to densely packed (Fig. 1F, H, J). The border between these nuclei was often difficult to determine.

The anterior pulvinar nucleus (PA) was located between the VP complex and CM. The PA reacted lightly for CO (Fig. 1G, I) and was observed to contain lightly stained, loosely packed small cells in the Nissl (Fig. 1H, J). The medial pulvinar (PM) was observed dorsal to PA and dorsolateral to CM. PM was lightly to moderately reactive to CO and contained small- to medium-sized neurons that were moderately stained for Nissl (Fig. 1I–L). In both CO

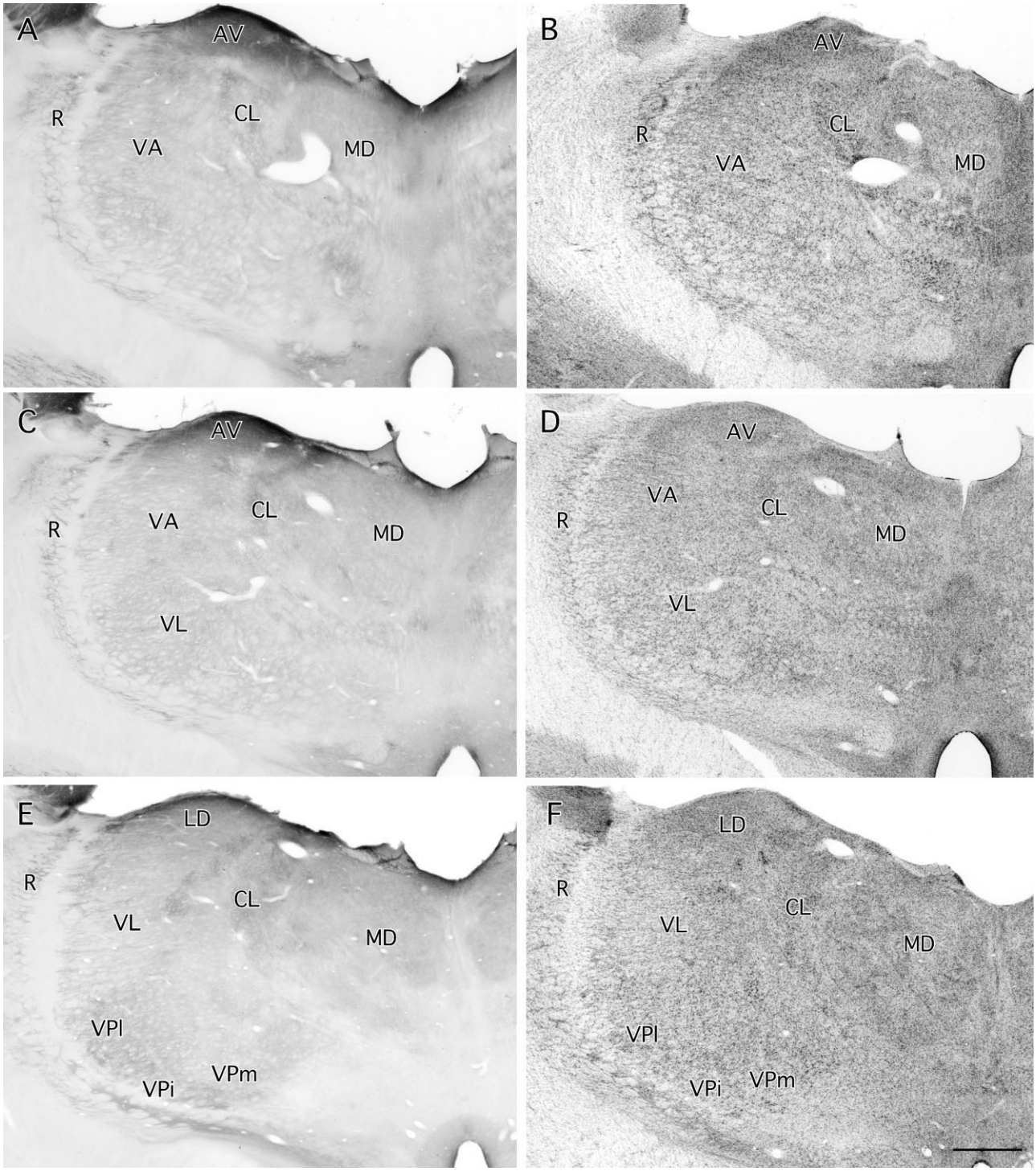

Fig. 1. Digital images of coronal sections from rostral (**A, B**) through caudal (**K, L**) levels of the thalamus. These lightfield digital images of the thalamus are from case 01-79, and have been reacted for CO (**A, C, E, G, I, K**) and stained for Nissl (**B, D, F, H, J, L**). In rostral sections of the thalamus, AV, VA, VL, CL, and MD can be readily identified in either or both CO and Nissl stains (A–F). Caudally, VPs, VPm, VPl, VPi, PL, PM, and PA are distinct in either or both stains (G–L). The borders between some nuclei such as LD and LP are often difficult to determine (G, H). Arrowheads in panel G and H indicate septa separating VPm and VPl. Medial is up, lateral is to the left. Sections are 450 μm apart. Scale bar is 1 mm. See abbreviations list.

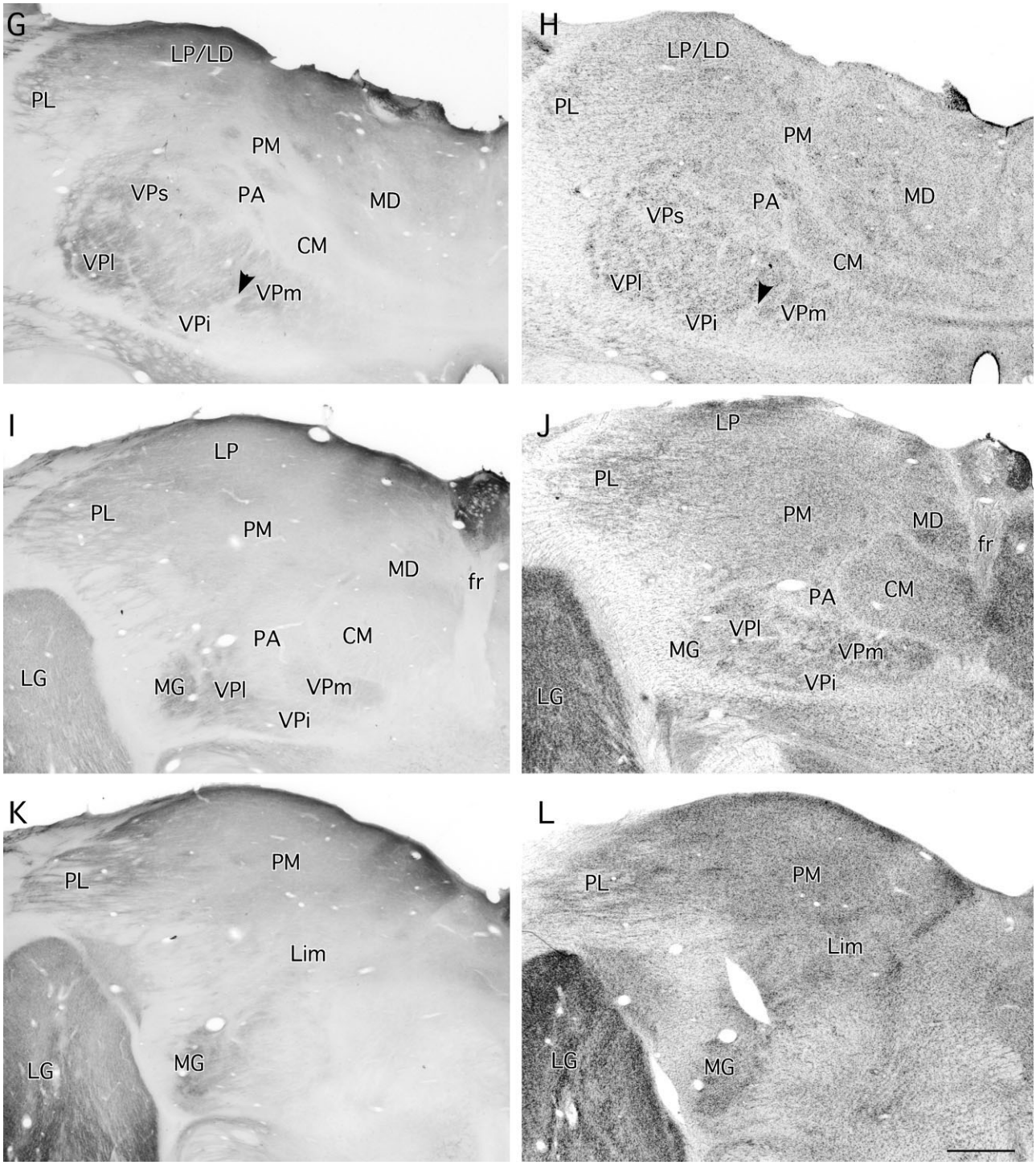

Figure 1 (Continued)

and Nissl, PM was observed to be relatively homogeneous. The lateral division of the pulvinar (PL) was located along the lateral edge of the caudal thalamus, and reacted strongly to CO (Fig. 1G, I, K). PL contained medium-sized neurons that stained darkly for Nissl (Fig. 1H, J, L). In both CO and Nissl, fibers appeared to fragment the nucleus. Caudally, the nucleus limitans (Lim) was located lateral to the superior colliculus (Fig. 1K, L). Lim reacted lightly to CO, and contained large, densely packed neurons that stained darkly for Nissl.

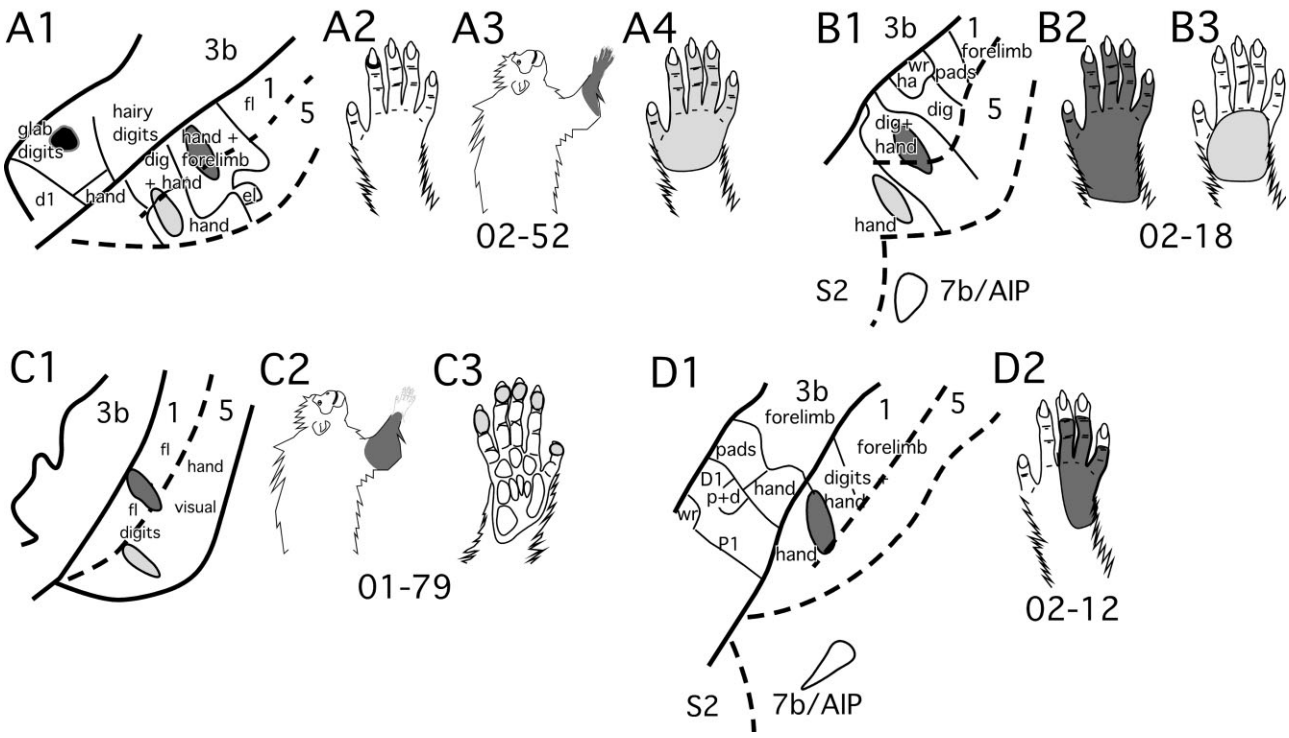

Fig. 2. Schematic diagrams of the electrophysiological responses at the locations of the mapped injection sites in the present study. Although not shown here, the maps of body part representations within cortical fields were obtained from multiple electrode penetrations in each area (see Padberg et al., 2005 for details). In case 02-52, biotinylated dextran amine (BDA) was injected into the d2 nailbed representation of area 3b, fluororuby (FR) was injected into the hand and forelimb representation in area 1, and fluoroemerald (FE) was injected into the dorsal hand representation in area 5 (A1–A4). In case 02-18, FR was injected into the dorsal hand representation of area 1, FE was injected into a partial dorsal hand representation in area 5, and BDA was injected into 7b/AIP (B1–B3). In case 01-79, FR was injected into the forelimb representation in area 1, and FE was injected into the distal digit tips representation in area 5 (C1–C3). In case 02-12, FR was injected into a partial dorsal hand representation in area 1, and BDA was injected into 7b/AIP (D1, D2). Black fill indicates 3b injection and receptive field, dark gray fill indicates area 1 injections and receptive fields, light gray fill indicates area 5 injections and receptive fields, and white fill indicates 7b/AIP injection. See abbreviations list and Table 1 for injection details.

Neuroanatomical tracer injections

Electrophysiological recording techniques were used to assess the receptive fields within or surrounding the injection sites in areas 3b, 1, and 5. In four animals, one injection was made into the d2 nailbed representation of area 3b (Fig. 2A1, A2), four injections were made into forelimb, hand, or partial hand representations in area 1 (Fig. 2A1, A3; B1, B2; C1, C2; D1, D2), three injections were made into the digit tips or hand representation of area 5 (Fig. 2A1, A4; B1, B3; C1, C3), and two injections were made in area 7b/AIP (Fig. 2B1, D1; Table 1). Representative injection sites and resulting label are shown in Figure 3.

Thalamic connections of area 3b

BDA was injected in the d2 nail bed representation in area 3b in case 02-52 (Fig. 2A1, A2). This injection resulted in many labeled cells and terminal fields in VPl (Fig. 4A–F). The labeled cells observed in VPl formed two patches, one that clustered tightly in the ventromedial aspect of the nucleus, in the expected location of the hand representation, and the other slightly dorsal to this (Fig. 4C). Anterograde terminal fields overlapped the clusters of cells (Fig. 4B–F). In addition, a few labeled neurons were observed in PA (Fig. 4E) and CL (Fig. 4C), although no terminal label was present in these nuclei.

Thalamic connections of area 1

In four cases, neuroanatomical tracers were placed in the electrophysiologically defined hand or forelimb representation of area 1 (Table 1; Fig. 2A1, A3; B1, B2; C1, C2; D1, D2). In cases 02-52 and 02-18, the injection into area 1 encroached slightly into area 5, but the overall pattern of thalamic label for this case is similar to the other cases with area 1 injections, suggesting that the major uptake was in area 1 (Fig. 2A1). In all of these cases, the resulting label in the thalamus was similar, although some variations were present (Figs. 5, 6). In case 02-52, an injection placed into the distal forelimb representation resulted in dense zones of labeled neurons in VL and PA (Fig. 5B–D). Less-dense groups of labeled neurons were observed in VPs and VPl (Fig. 5C–F). A few labeled neurons were observed in CL (Fig. 5A, C). In case 02-18, the injection into the dorsal hand representation resulted in labeled neurons predominantly in VL, PA, and VPs (Fig. 6). A few labeled cells were observed in the dorsal portion of VPl (Fig. 6C–E) and in CL (Fig. 6B, C). Two small zones of anterogradely

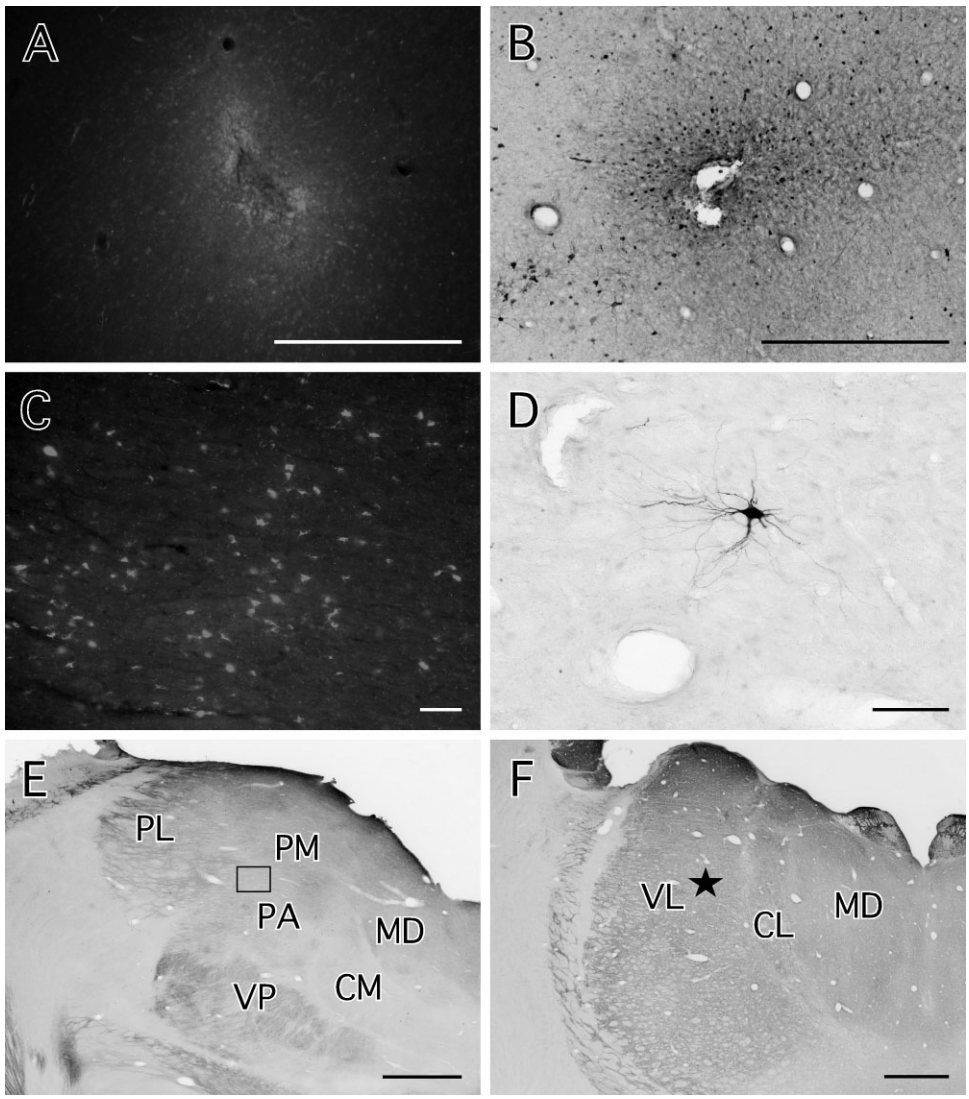

Fig. 3. Digital images of representative neuroanatomical tracer injections (**A, B**); resulting labeled cells in the thalamus (**C, D**); the relationship of the cells in C and D to architectonic divisions of the thalamus (**E, F**). **A:** FR injection site in area 1 of case 01-79. Scale bar is 500 μm. **B:** BDA injection site in area 7b/AIP of case 02-18. Scale bar is 500 μm. **C:** FR-labeled cells in PA in case 01-79. Scale bar is 500 μm. **D:** BDA-labeled cell in VL in case 02-18. Scale bar is 100 μm. **E:** CO-reacted section adjacent to section shown in panel B. Box indicates location of cells shown in panel C. Scale bar is 1 mm. **F:** CO-reacted section adjacent to section shown in panel D in case 02-18. Black star indicates location of cell shown in panel D. Scale bar is 100 μm.

labeled terminals were observed in PA (Fig. 6E, F) and VPl (Fig. 6D). In case 01-79 (not shown), an injection into the forelimb representation resulted in labeled neurons predominantly in VL, PA, VPs, and PM. A few labeled neurons were observed in VPl, CL, CM, MD, and the nucleus limitans. In case 02-12 (not shown), an injection into a partial hand representation resulted in many labeled neurons in VL and VA. A few labeled cells were also observed in PA, LP, and CL. The area 1 injections in cases 02-52 and 01-79 resulted in more dense and widespread thalamic label than did cases 02-18 and 02-12. Taken together, the most consistent finding was that area 1 received dense convergent inputs from VL, PA, and VPs, and moderate to sparse inputs from VPl and CL.

Thalamic connections of area 5

In three cases, injections were made into area 5 (Table 1; Fig. 2A1, A4; B1, B3; C1, C3). In case 02-52, the injection into area 5 encroached slightly into area 1, but the overall pattern of thalamic label for this case is similar to the other cases with area 5 injections, suggesting that the major uptake was in area 5. The extent of the resulting thalamic label in all cases was more widespread than the labeled cells observed after injections into areas 3b and 1. In case 01-79, an injection into the digit tips representation of area 5 resulted in widespread thalamic label with the densest zones in VL, PA, and PM (Fig. 7B–D). The CL nucleus, VPl, and VPs were moderately labeled (Fig. 7C, D), and a few cells were observed in VA, CM, and the

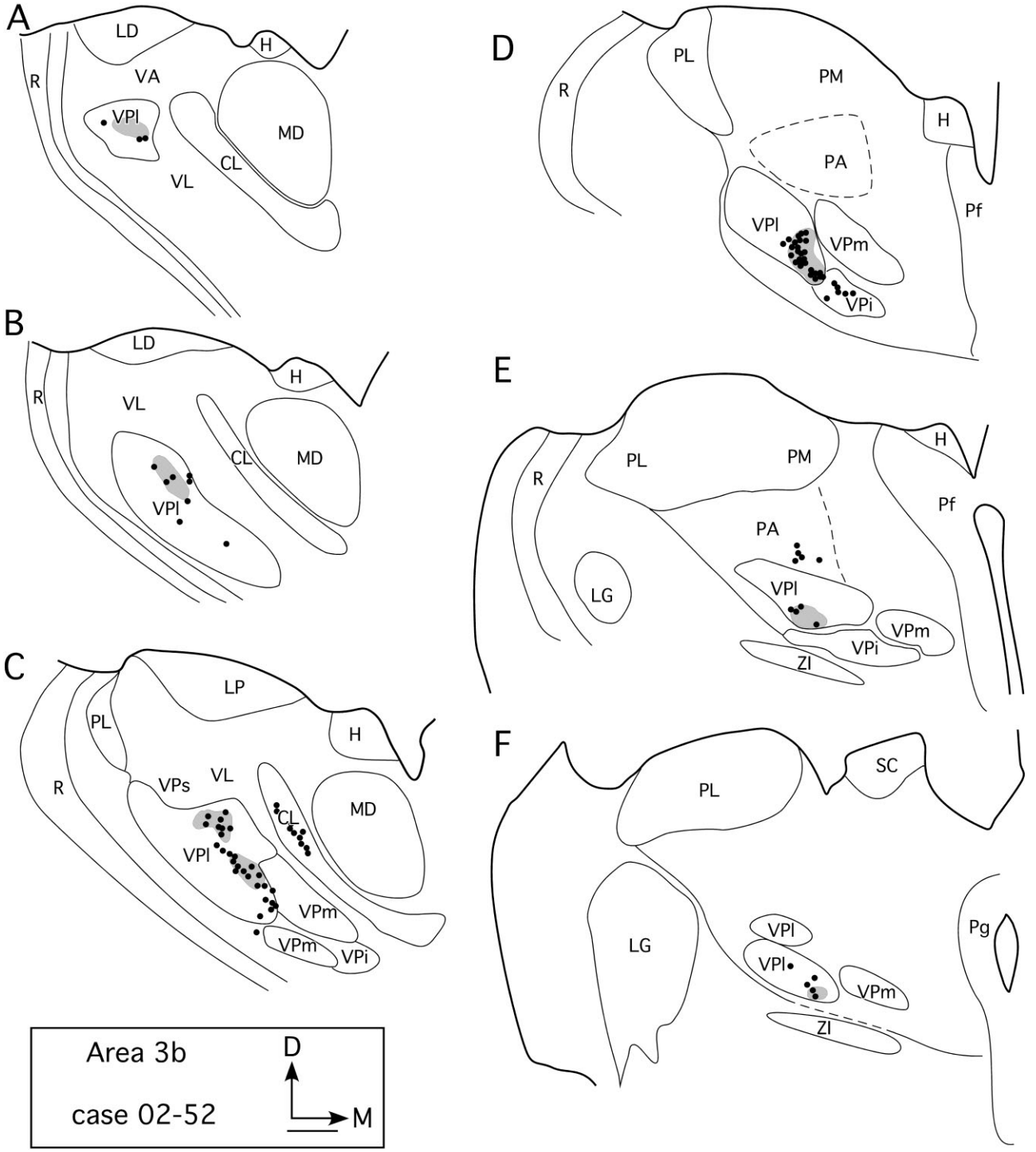

Fig. 4. Reconstruction of a coronally cut series of sections through the thalamus for case 02-52 (**A–F**). In this case, an injection of BDA was placed in the D2 nailbed representation of area 3b (Fig. 2A). The resulting locations of labeled cell bodies relative to thalamic nuclei boundaries are shown. Black filled circles represent BDA-labeled cells and gray crosshatching represents anterograde terminal fields resulting from the BDA injection. Most of the labeled cells and anterograde terminals from the 3b injection were observed within VPl. A small cluster of labeled cells was observed in CL and PA. Thin lines denote boundaries of thalamic nuclei, determined based on CO reactivity. In this and the following figures, the series of sections run from rostral (A) through caudal (F or G). Scale bar is 1 mm. Other conventions as in previous figures.

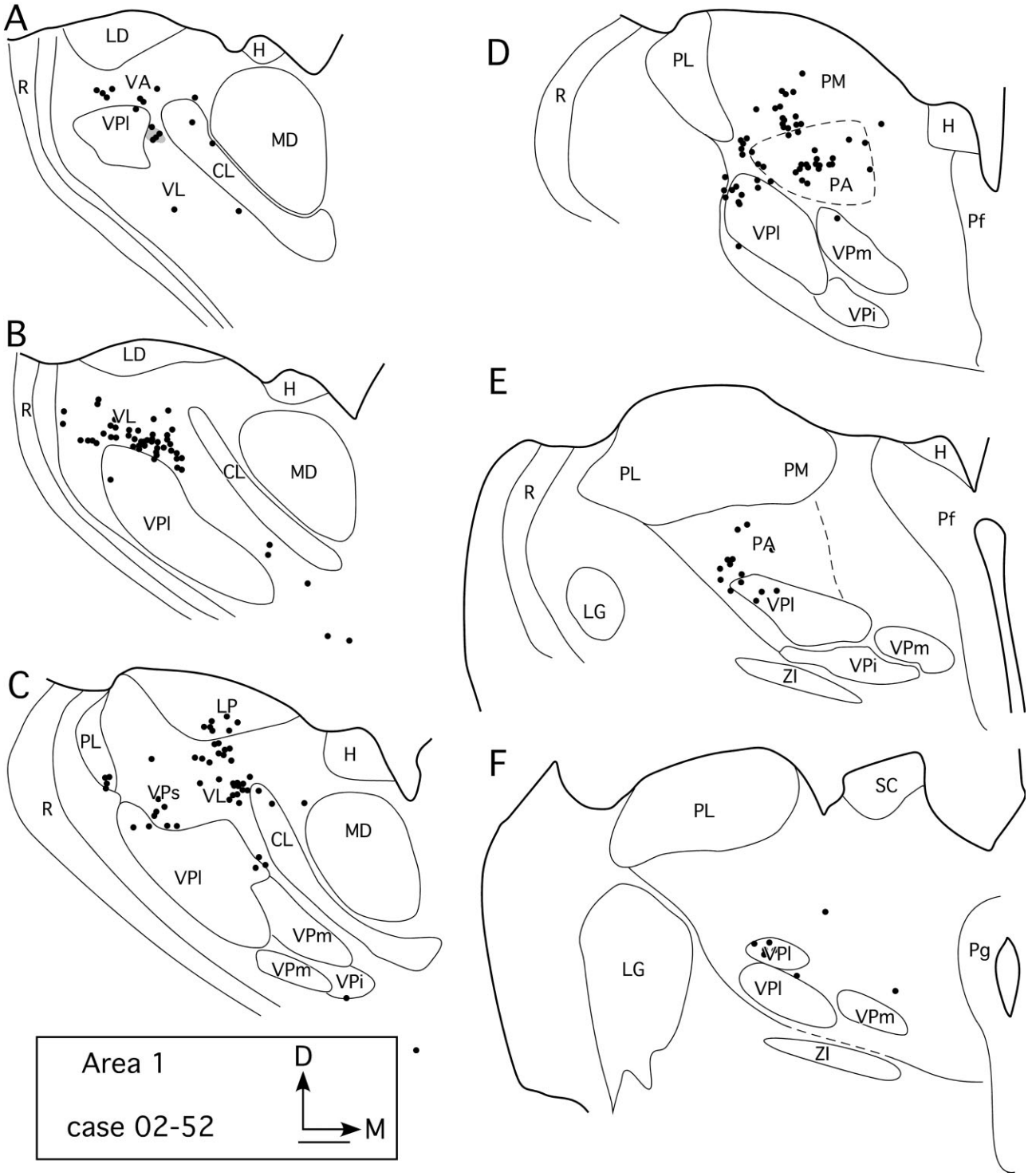

Fig. 5. Reconstruction of coronally cut series of sections through the thalamus for case 02-52 (**A–F**). In this case, an injection of FR was placed in the distal forelimb representation of area 1 (Fig. 2A). Most of the labeled cells resulting from the FR injection were observed in VL and PA. Less dense labeled cells were observed in VPs and VPl. A few labeled cells were in CL. Thin lines denote boundaries of thalamic nuclei, determined based on CO reactivity. Conventions as in previous figures.

limitans (Fig. 7). In case 02-52, an injection into the dorsal hand representation (Fig. 2D) resulted in widespread label in the thalamus, similar to the patterns observed for case 01-79 (Fig. 8). The densest regions of labeled neurons were in VL, PA, PM, and VPl (Fig. 8B–F). Labeled cells in VPl were in the lateral portion of the nucleus at rostral

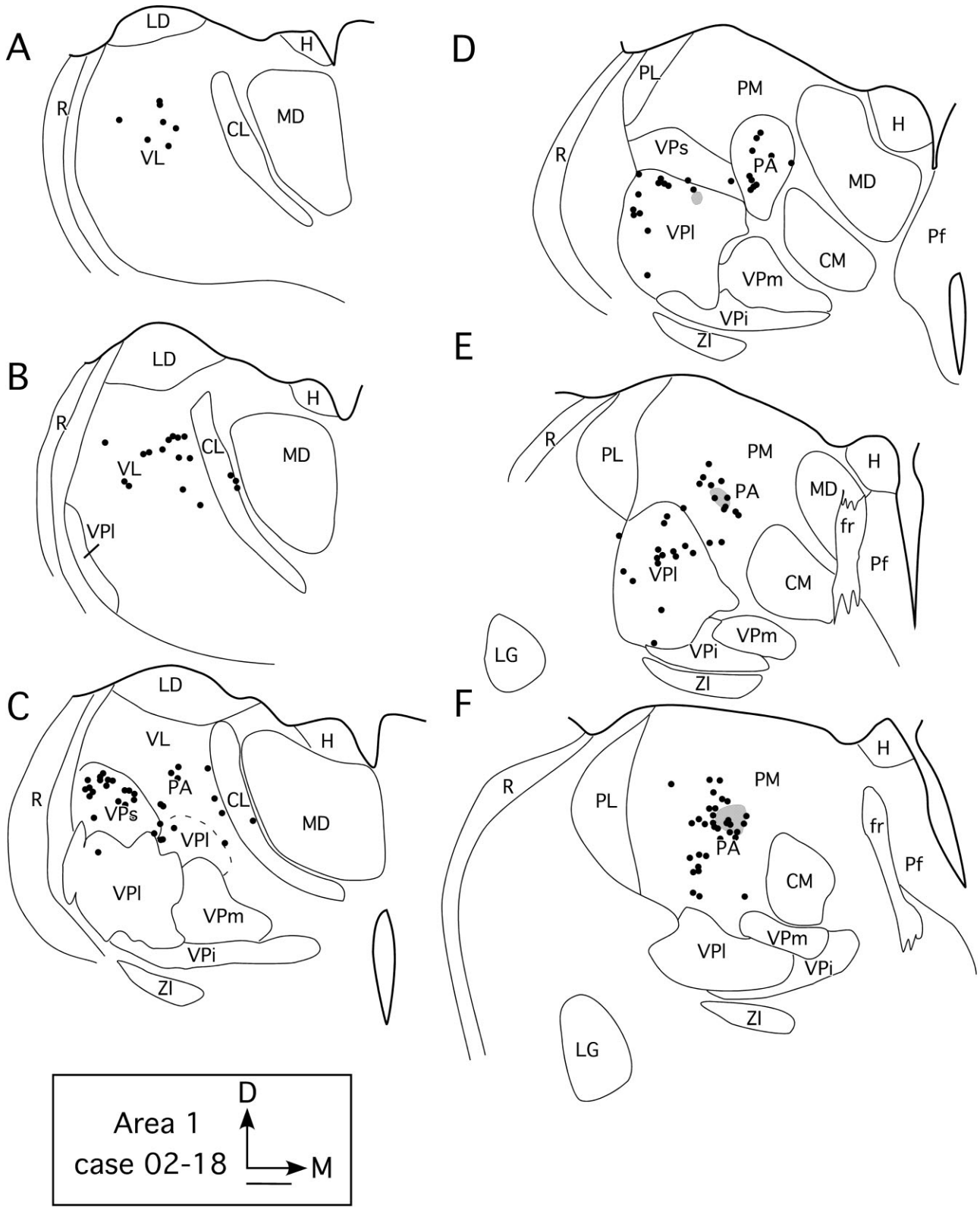

Fig. 6. Reconstruction of coronally cut series of sections through the thalamus for case 02-18 (**A–F**). In this case, an injection of FR was placed in the distal hand representation of area 1 (Fig. 2B). Most of the labeled cells resulting from the FR injection were observed in VL, VPs, and PA (B–F). Zones of anterograde label are located in PA and VPl. A few cells were observed in CL. Thin lines denote boundaries of thalamic nuclei, determined based on CO reactivity and Nissl staining. Dashed lines denote approximate borders. Conventions as in previous figures.

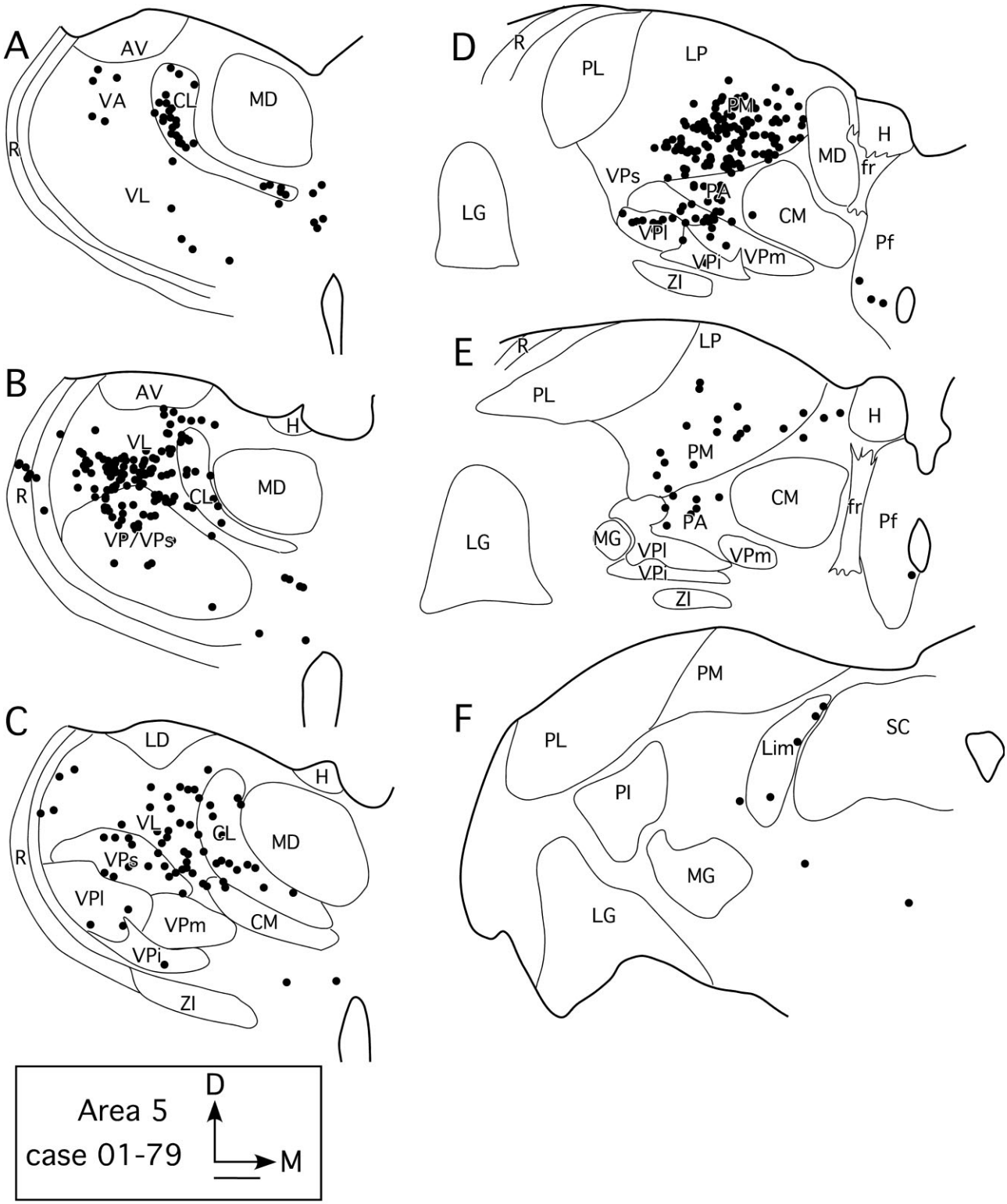

Fig. 7. Reconstruction of a coronally cut series of sections through the thalamus for case 01-79 (**A–F**). In this case, an injection of FE was placed in the distal digit tip representation of area 5 (Fig. 2C). Most of the labeled cells resulting from the FE injection were observed in VL, PA, and PM, with moderate density of labeled cells in CL, VPs, and VPl. Sparse label was observed in the nucleus limitans, CM, and VPi. Thin lines denote boundaries of thalamic nuclei, determined based on CO reactivity and Nissl staining. Conventions as in previous figure.

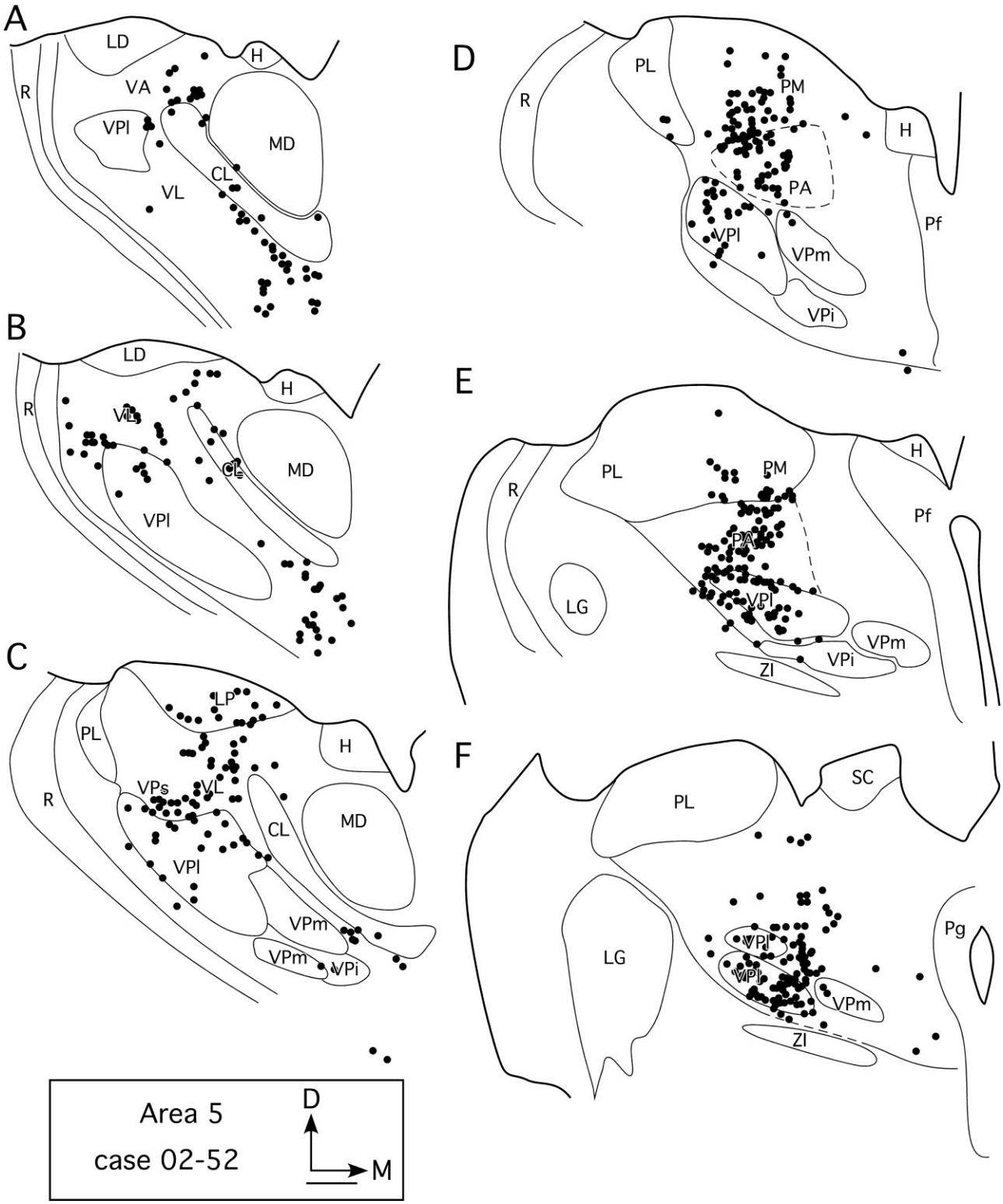

Fig. 8. Reconstruction of a coronally cut series of sections through the thalamus for case 02-52 (**A–F**). In this case, an injection of FE was placed in the hand representation of area 5 (Fig. 2D). Most of the labeled cells resulting from the FE injection were observed in VL, PA, PM, VPs, and VPl (B–F). Labeled cells in VPl were observed in the lateral portion of the nucleus rostrally and filled the nucleus caudally. Less dense labeled cells were observed in CL and LP. Thin lines denote boundaries of thalamic nuclei, determined based on CO reactivity. Scale bar is 1 mm.

levels, and filled the nucleus caudally (Fig. 8F). Moderately dense labeled cells were observed in VPs, CL, and LP. In case 02-18, an injection into the dorsal hand representation (not shown) resulted in densely labeled neurons that were in VL, VPs, and PA. The VPl nucleus and PM were moderately labeled, and CL contained a few labeled neurons. Anterograde terminal fields were also observed in VL and VPl. Taken together, the thalamic connections of area 5 are broadly distributed and highly convergent from a number of thalamic nuclei including VL, VPl, VPs, PA, and PM. Sparse projections arise from CL, and inconsistent label was observed in LP and the limitans.

Thalamic connections of area 7b/AIP

Injections of BDA were made in area 7b/AIP in two cases (Fig. 2B1, D1). These injections were made relative to sulcal patterns and the injection sites were not mapped. In both cases, dense to moderate projections were from PA, PM, LP, and VL (Figs. 9, 10). In both cases, terminal fields were also observed in PA, PM, and LP/LD. Sparse connections were observed with CL, PL, and CM. Similar to area 5, 7b/AIP receives highly convergent connections from a number of thalamic nuclei.

DISCUSSION

Thalamocortical connections of anterior parietal areas 3b and 1 in New World and Old World monkeys

Thalamocortical connections of area 3b have been well studied in primates. Without exception, the major source of thalamic input to area 3b in both New World (e.g., Coq et al., 2004; Cusick and Gould, 1990; Krubitzer and Kaas, 1992; Lin et al., 1979; Mayner and Kaas, 1986) and Old World monkeys (e.g., Darian-Smith et al., 1990; e.g., Jones et al., 1979; Nelson and Kaas, 1981) is the VP, which receives low threshold cutaneous inputs from the contralateral face and body (e.g., Kaas et al., 1984; Loe et al., 1977; Rausell and Jones, 1991). Studies in which injection sites in 3b are highly restricted demonstrate some small differences in the patterns of thalamocortical connections of area 3b in New World versus Old World monkeys (Fig. 11A–C). In Old World monkeys, VP is the only nucleus in the dorsal thalamus that projects to area 3b (e.g., Jones et al., 1979; Nelson and Kaas, 1981). Although the predominant input to area 3b in all New World monkeys is VP, sparse thalamocortical projections also arise from the anterior pulvinar, and in some cases, VPs, VL, and CL (e.g., Cusick and Gould, 1990; Krubitzer and Kaas, 1992). The only exception to this is the Cebus monkey, in which the pattern of highly restricted thalamocortical connections to area 3b from the VP is identical to that of macaque monkeys (Mayner and Kaas, 1986). In galagos, thalamocortical connections to S1 appear even more widespread than in New World monkeys and include VP, VIM, VL, CM, CL, and PO (Pearson and Haines, 1980). However, the HRP pellets implanted in S1 in these studies resulted in a very large "injection" site, which may have included motor cortex. In the current investigation, we demonstrate that area 3b receives dense input from VP and sparse input from the anterior pulvinar, as has been demonstrated previously in titi monkeys (Coq et al., 2004). We also observed sparse connections with CL.

The connections of area 1 in macaque monkeys, as demonstrated by placing small injections into electrophysiologically defined body part representations, are very similar to those of area 3b in that the VP serves as the major source of thalamic input to area 1 (Nelson and Kaas, 1981; Pons and Kaas, 1985), although sparse connections with VPs have also been reported (Pons and Kaas, 1985). Thalamocortical connections of area 1 appear to be different in different groups of New World monkeys. For instance, in New World monkeys in which area 1 has been well defined using electrophysiological recording techniques, and in which the topographic organization of the field is distinct, such as Cebus monkeys (Mayner and Kaas, 1986), owl monkeys (Lin et al., 1979), and squirrel monkeys (Cusick and Gould, 1990), the thalamocortical connections of area 1 are strikingly similar to those in macaque monkeys (Fig. 11A, B). Thus, VP provides the major source of input to the field with inconsistently and sparse input from a region of the thalamus just dorsal to VP, VPs. For the squirrel monkey, sparse input has also been reported from PA, but the injection in area 1 in this study was large and appears to have included cortex caudal and rostral to area 1 (Cusick and Gould, 1990).

In other New World monkeys, such as titi monkeys (Coq et al., 2004, and the current study), thalamocortical connections of area 1 appear to be more widespread and are dense with VL, VPs, PA, and sparse with VPl (Fig. 11C). As noted above, VP receives cutaneous input. The VPs, however, processes inputs from deep receptors of the skin and joints (e.g., Asanuma et al., 1983; e.g., Dykes et al., 1981; Friedman and Jones, 1981; Kaas et al., 1984), and VL is associated with the motor system (Asanuma et al., 1983; Gonzalo-Ruiz and Leichnetz, 1990; Ilinsky and Kultas-Ilinsky, 2002; Kultas-Ilinsky et al., 2003; Stepniewska et al., 1994b; Vitek et al., 1994; Vitek et al., 1996). The anterior pulvinar is a nucleus associated with somatic processing (e.g., Asanuma et al., 1985; Cusick and Gould, 1990; see Grieve et al., 2000 for review; Jones et al., 1979; Pons and Kaas, 1985).

The different thalamocortical connections of area 1 may have to do with the status of this field in each monkey. In squirrel monkeys, Cebus monkeys, and owl monkeys, area 1 has a very precise topographic organization, and the neurons have very small receptive fields and respond exclusively to cutaneous stimulation of the contralateral body (Felleman et al., 1983; Merzenich et al., 1978; Sur et al., 1982). In titi monkeys, the topographic organization of area 1 is less precise, and receptive fields for neurons are relatively large (e.g., see Fig. 3 in Padberg et al., 2005). Furthermore, some neurons in area 1 in titi monkeys respond to stimulation of deep receptors, and in a few instances, to visual stimulation. Thus, it appears that the high topographic precision and small receptive fields in area 1 in some primates, such as macaque, owl, Cebus, and squirrel monkeys, are the result of highly restricted, nonconvergent inputs from VP (Fig. 11A, B). In other primates in which area 1 is less precisely organized and less modality specific, such as the titi monkey, thalamocortical connections are highly convergent from nuclei associated with cutaneous and deep somatic inputs, and motor processing (Fig. 11C). This observation has important implications for understanding the magnitude of the contribution of thalamic inputs to receptive field characteristics and features of cortical field organization compared with intrinsic and extrinsic corticocortical connections.

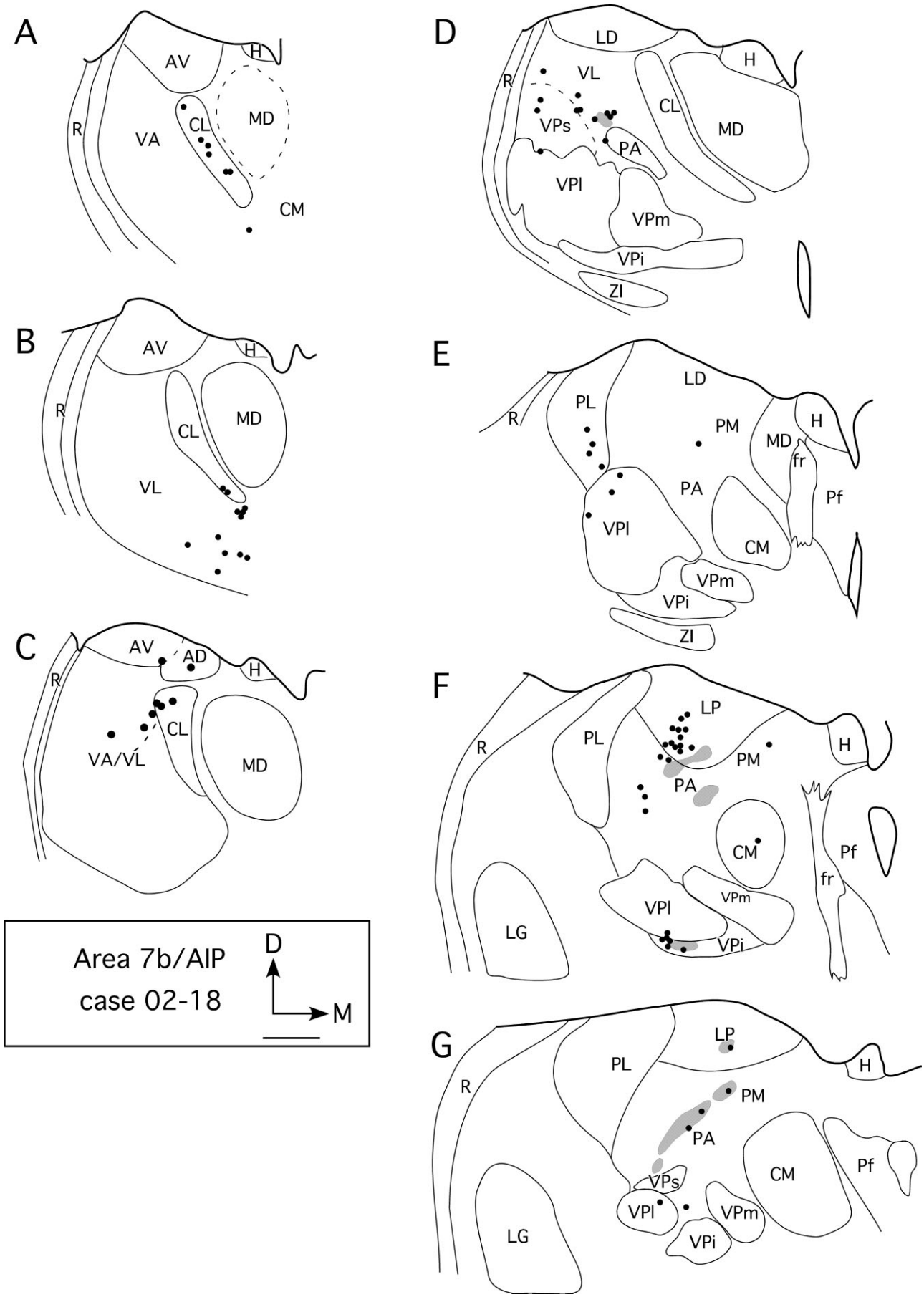

Fig. 9. Reconstruction (**A–G**) of a coronally cut series of sections through the thalamus for case 02-18 in which area 7b/AIP was injected with BDA. Black filled circles represent BDA-labeled cells resulting from an injection into 7b/AIP and outlined crosshatching represents anterograde terminal fields. Most of the labeled cells resulting from the 7b/AIP injection were observed in PM, PA, and LP, with terminal fields located in PM, PA, and LP. A few scattered cells were also observed in CL, CM, and VPi. Thin lines denote boundaries of thalamic nuclei, determined based on CO reactivity and Nissl staining. Conventions as in previous figure.

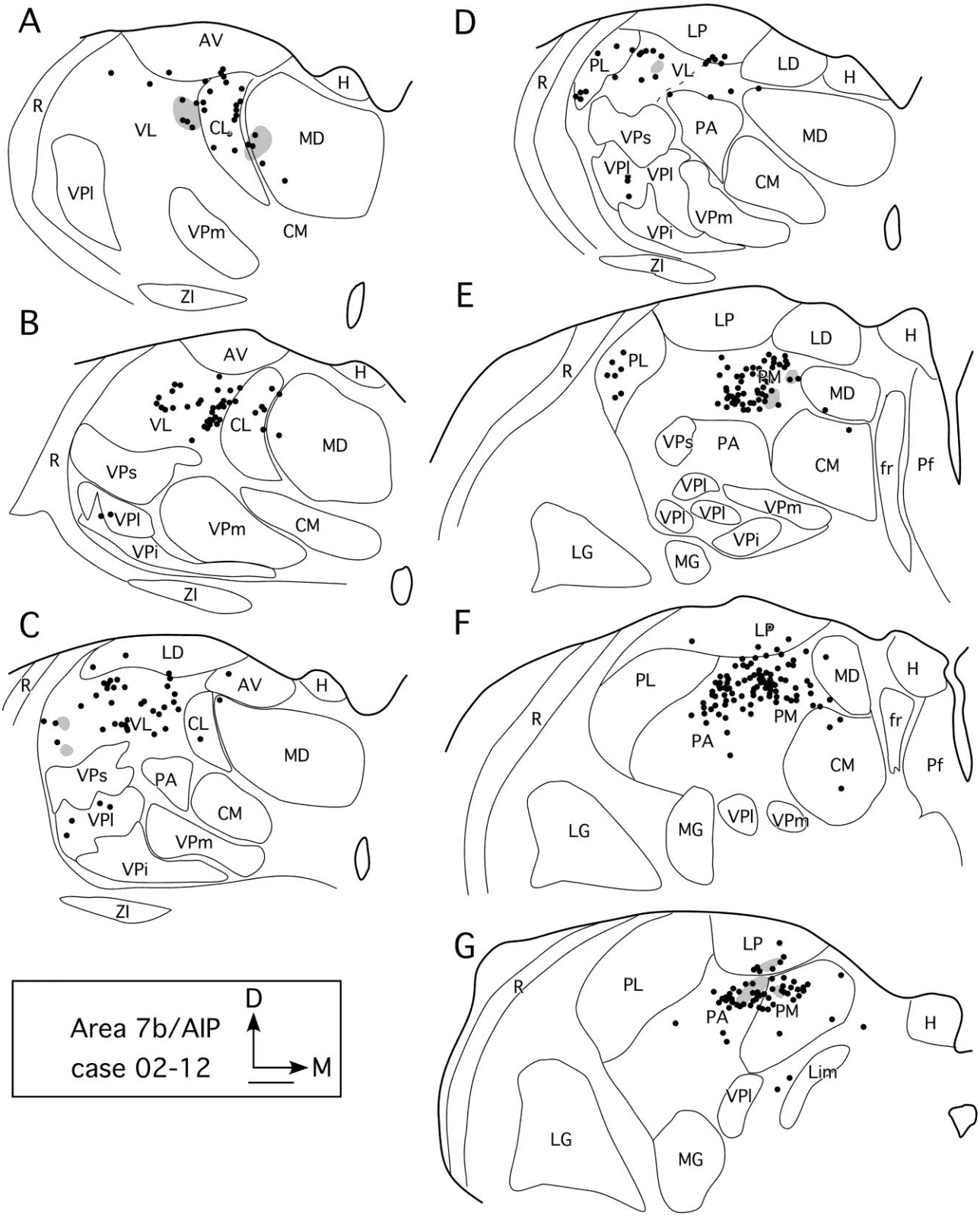

Fig. 10. Reconstruction (**A–G**) of a coronally cut series of sections through the thalamus for case 02-12 in which area 7b/AIP was injected with BDA. Outlined crosshatching represents anterograde terminal fields resulting from the BDA injection. Most of the cells and anterograde terminals were observed in PM, PA, VL, and LP. Terminal fields were observed in PM, PA, LP, and VL. Scattered cells were observed in CL, CM, and MD. Thin lines denote boundaries of thalamic nuclei, determined based on CO reactivity and Nissl staining. Conventions as in previous figures.

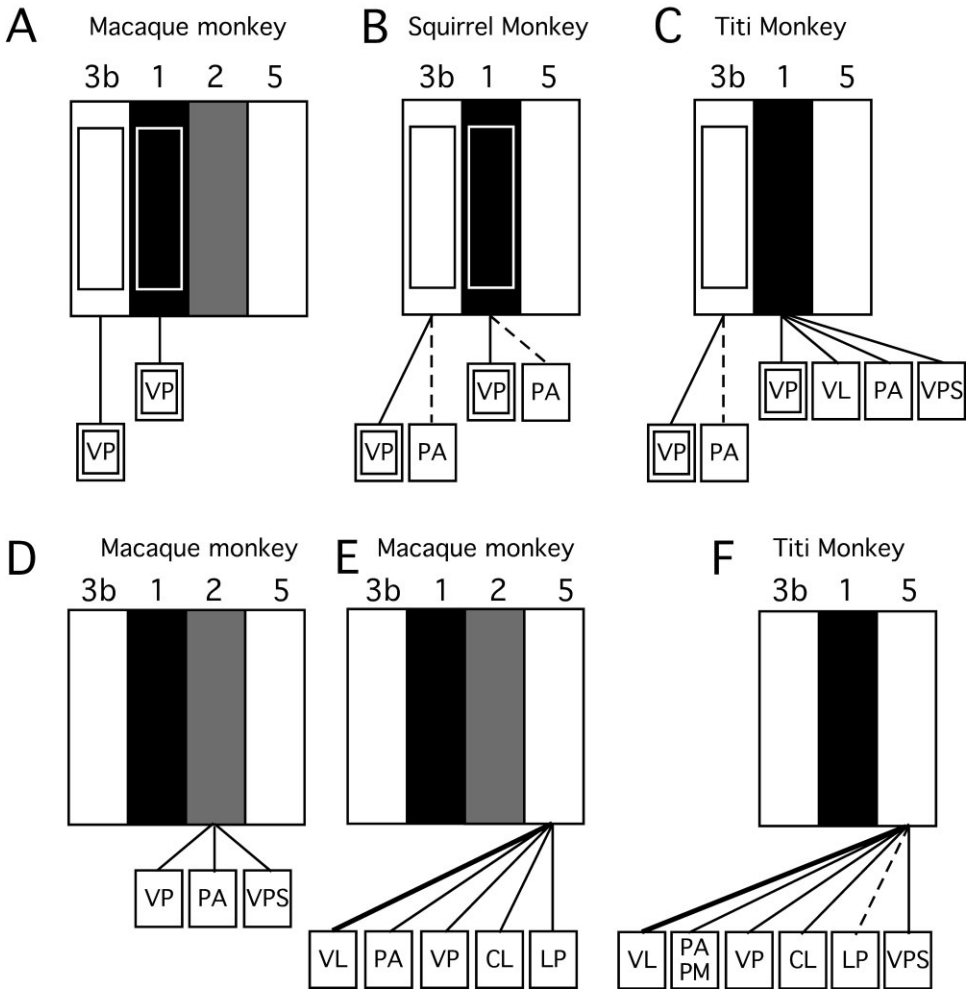

Fig. 11. Summary diagram of thalamocortical projections to parietal areas of Old World and New World monkeys. The high topographic precision within areas 3b and 1 in macaque (**A**; Jones et al., 1979) and squirrel monkeys (**B**; Cusick and Gould, 1990; Sur et al., 1982) is the result of highly restricted inputs from VP. In species such as titi monkeys that have a less precisely organized area 1 (solid black), thalamocortical projections are highly convergent from nuclei associated with cutaneous and deep somatic inputs and motor processing (**C**; Coq et al., 2004; present study). Boxes within VP and areas 3b and 1 indicate precise topography. The thalamocortical connections of cortex caudal to area 1 in titi monkeys are more similar to the thalamocortical connections in area 5, rather than area 2, of macaques (**D–F**; Jones et al., 1979; Pons and Kaas, 1985; Schmahmann and Pandya, 1990; Yeterian and Pandya, 1985). Thalamocortical connections of area 2 in macaques originate mainly from VP, VPs, and PA (D). Thalamocortical connections of area 5 in macaques originate mainly from VL, PA, VPl, CL, and LP (E). Thicker lines from VL indicate most dense connections. In titi monkeys, the thalamocortical connections of cortex caudal to area 1 were similar to that of macaque area 5, and originated mainly from VL, PA, VPl, CL, VPS, and PM (F). Thicker lines from VL indicate most dense connections.

Thalamocortical connections of cortex caudal to area 1 in New World and Old World monkeys

The status of area 2 in New World monkeys is questionable from both an electrophysiological and anatomical viewpoint. In a previous investigation on cortical organization and connections in titi monkeys, we found no evidence for an area 2 using a variety of criteria including electrophysiological recording techniques, cortical connections, and cortical architecture (Padberg et al., 2005). Our examination of data from previous studies on cortex posterior to area 1 in New World monkeys and prosimian galagos revealed much the same (see Padberg et al., 2005 for full discussion), in that this region has only been explored in a very limited manner, and the number of recording sites in different monkeys was small or not illustrated (e.g., Krubitzer and Kaas, 1990, marmosets; Merzenich et al., 1978, owl monkeys; Sur et al., 1982, squirrel monkeys). When the data have been shown, most neurons were either unresponsive or responsive to high-threshold stimulation, often of the hand. In our study in titi monkeys, this region of cortex was dominated by neurons responsive to stimulation of deep receptors of the hand and forelimb, and often to visual stimulation, much like area 5 in macaque monkeys (e.g., Disbrow et al., 2001; see Iwamura, 2000 for review; Iwamura et al., 1994; Iwamura et al., 2002; Mountcastle et al., 1975; Sakata et

al., 1973; Taoka et al., 2000). Furthermore, cortical connections were widespread, particularly with posterior parietal visual areas in the IPS, and motor areas of frontal cortex, such as M1 and PM. After reexamination of all previous data regarding areas 1, 2, and 5 in both New World and Old World monkeys, we concluded that New World monkeys did not appear to possess an area 2.

In the present investigation, thalamocortical connections of this region of cortex immediately caudal to area 1 support the contention that area 2 is not present. In macaque monkeys in which injection sites in area 2 have been electrophysiologically determined, the primary source of thalamic input to area 2 is from the superior division of VPS, PA, and VP (Pons and Kaas, 1985; Fig. 11D). In the present investigation, this region of cortex had dense interconnections with rostral regions of the thalamus, including VL, and with subdivisions of the pulvinar (PA and PM; see Results for details). These connections are similar to those described for area 5 in macaque monkeys (Fig. 11D–F; also see below). Taken together, both recent work in our laboratory in the titi monkey (Padberg et al., 2005), as well as a reexamination of electrophysiological and anatomical data from this region of cortex in other New World monkeys (see above and also Padberg et al., 2005, for review of this data), indicate that cortex caudal to area 1 is markedly different than that of area 2 described in Old World macaque monkeys. We propose that area 2 is a cortical field that arose in the lineage that led to modern anthropoid monkeys and apes (including humans), and may be associated with the coevolution of the opposable thumb. If this is the case, one might expect New World monkeys that have independently evolved an opposable thumb, such as Cebus monkeys, to have a similar organization of anterior parietal cortical areas to macaque monkeys, including the presence of an area 2.

Thalamocortical connections of posterior parietal area 5 and 7b/AIP: Motor or sensory?

Previous studies of thalamocortical connections of area 5 in macaque monkeys indicate that nuclei located in rostral portions of the dorsal thalamus, generally associated with motor processing (e.g., Vitek et al., 1994; Vitek et al., 1996), provide input to this field. For example, injections in the rostral bank of the IPS in the location of area 5 (Jones et al., 1979; Schmahmann and Pandya, 1990; Yeterian and Pandya, 1985), or in one case, in a physiologically defined location in area 5 (Pons and Kaas, 1985), demonstrated projections from VL, PA, VPl, CL, and LP (Fig. 11E). As noted above, similar patterns of thalamocortical connections are observed for area 5 in the present study in titi moneys in that area 5 is interconnected with VL, PA, and VPl, with additional input from CL, VPs, and PM (Fig. 11F). We found data from only one other study in New World owl monkeys (Lin et al., 1979) in which one injection was placed in cortex immediately caudal to area 1. In this study, connections were relatively restricted, but the major source of thalamic input to this region was VL, much like that of the present investigation, and like area 5 in macaque monkeys.

In macaque monkeys, AIP is a region of cortex associated with visually guided hand movements (see Andersen and Buneo, 2002 for review; Cavada, 2001; Luppino et al., 1999; Murata et al., 2000; Sakata et al., 1995). We have previously argued (Padberg et al., 2005) that, based on connections, AIP and 7b in macaque monkeys were indistinguishable and may actually compose the same field. The thalamocortical connections of electrophysiologically identified locations in areas AIP and 7b have not been directly examined in macaque monkeys, or any other primate. However, cortex in the location of what in modern terms is called AIP and 7b, have been examined in previous studies in which sulcal patterns were used to determine the location of injection sites. For example, Yeterian and Pandya (1985) and Schmahmann and Pandya (1990) placed injections of radioactive proline or WGA-HRP respectively into cortex at the lateral tip of the IPS, in the location of AIP, and in some cases including cortex in the location of 7b. Connections were with the paracentral nucleus (PC), CL, MD, VL, VP, VPi, LP, and the posterior group (PO) for the more restricted injection and with these nuclei as well as PO and PM, PL and VL in the injections that were larger (e.g., see case 12, Yeterian and Pandya, 1985). In the current investigation in New World titi monkeys, thalamocortical connections of 7b/AIP were most dense with PM and PA, and less dense with PL, VL, CM, CL, and LD/LP. It is difficult to make accurate comparisons between data sets in titi and macaque monkeys because injection sites in both were based on sulcal patterns. However, the preponderance of thalamic connections from the pulvinar and motor nuclei of the thalamus supports the role of 7b/AIP in titi monkeys in visual motor function.

Taken together, the data indicate that the field immediately caudal to area 1 in titi monkeys is homologous to area 5 in macaque monkeys, and that 7b/AIP may be homologous as well. Corticocortical connections of area 5, and to a more limited extent area 7b/AIP, are predominantly with motor areas of the neocortex including motor, premotor, and frontal eye movement fields (Jones et al., 1978; Jones and Powell, 1969; Padberg et al., 2005; Pandya and Seltzer, 1982; see Rizzolatti et al., 1998 for review). As discussed in the introduction, microstimulation of posterior parietal cortical areas, including area 5 (Cooke et al., 2003; Stepniewska et al., 2005), evoke ecologically relevant behaviors including defensive movements, hand to mouth movements, facial grimaces, and aggressive movements. Furthermore, studies of neural response properties and stimulus conditions in awake monkeys indicate that posterior parietal areas are involved in generating a body-centered coordinate system (Andersen and Buneo, 2002; Ferraina and Bianchi, 1994; Lacquaniti et al., 1995; Wise et al., 1997). Our results on thalamocortical connections of area 5 and 7b/AIP support the contention posed decades ago by Mountcastle et al. (1975), and the results from recent microstimulation studies by Graziano et al. (2002), Cooke et al. (2003), and Stepniewska et al. (2005), that these areas and other posterior parietal regions are sensorimotor areas of the neocortex. In primates, these areas are highly specialized and associated with species-specific behaviors of the hand and eyes, and differences may arise in different groups of primates based on the evolution of different hand morphologies, in particular, the evolution of an opposable thumb. If this is the case, then one might expect aspects of posterior parietal and even anterior parietal organization to diverge in each group. To some extent, the lack of an area 2 in primates without an opposable thumb supports this contention.

ACKNOWLEDGMENTS

The authors thank Katy Campi, Deborah Hunt, Sarah Karlen, and Gregg Recanzone for helpful comments on the manuscript.

LITERATURE CITED

Andersen RA, Buneo CA. 2002. Intentional maps in posterior parietal cortex. Annu Rev Neurosci 25:189–220.

Asanuma C, Andersen RA, Cowan WM. 1985. The thalamic relations of the caudal inferior parietal lobule and the lateral prefrontal cortex in monkeys: divergent cortical projections from cell clusters in the medial pulvinar nucleus. J Comp Neurol 241(3):357–381.

Asanuma C, Thach WT, Jones EG. 1983. Distribution of cerebellar terminations and their relation to other afferent terminations in the ventral lateral thalamic region of the monkey. Brain Res Rev 5:237–265.

Cavada C. 2001. The visual parietal areas in the macaque monkey: current structural knowledge and ignorance. Neuroimage 14:S21–S26.

Cavada C, Goldman-Rakic PS. 1989. Posterior parietal cortex in rhesus monkey. I. Parcellation of areas based on distinctive limbic and sensory corticocortical connections. J Comp Neurol 287:393–421.

Cooke DF, Taylor CS, Moore T, Graziano MS. 2003. Complex movements evoked by microstimulation of the ventral intraparietal area. Proc Natl Acad Sci USA 100(10):6163–6168.

Coq JO, Qi H, Collins CE, Kaas JH. 2004. Anatomical and functional organization of somatosensory areas of the lateral fissure of the New World titi monkey (*Callicebus moloch*). J Comp Neurol 476(4):363–387.

Cusick CG, Gould HJI. 1990. Connections between area 3b of the somatosensory cortex and subdivisions of the ventroposterior nuclear complex and the anterior pulvinar nucleus in squirrel monkeys. J Comp Neurol 292:83–102.

Darian-Smith C, Darian-Smith I, Cheema SS. 1990. Thalamic projections to sensorimotor cortex in the macaque monkey: use of multiple retrograde fluorescent tracers. J Comp Neurol 299:17–46.

Disbrow E, Litinas E, Recanzone G, Slutsky D, Krubitzer LA. 2002. Thalamocortical connections of the parietal ventral area (PV) and the second somatosensory area (S2) in macaque monkeys. Thalamus Relat Syst 1:289–302.

Disbrow E, Roberts T, Poeppel D, Krubitzer L. 2001. Evidence for interhemispheric processing of inputs from the hands in the human second somatosensory and parietal ventral areas. J Neurophysiol 85:2236–2244.

Disbrow E, Roberts TPL, Slutsky D, Krubitzer L. 1999. The use of fMRI for determining the topographic organization of cortical fields in human and nonhuman primates. Brain Res 829:167–173.

Dubowitz DJ, Chen DY, Atkinson DJ, Grieve KL, Gillikin B, Bradley WG Jr, Andersen RA. 1998. Functional magnetic resonance imaging in macaque cortex. Neuroreport 9(10):2213–2218.

Dykes RW, Sur M, Merzenich MM, Kaas JH, Nelson RJ. 1981. Regional segregation of neurons responding to quickly adapting, slowly adapting, deep and pacinian receptors within thalamic ventroposterior nuclei in the squirrel monkey (*Saimiri sciureus*). Neuroscience 6(8):1687–1692.

Emmers R, Akert K. 1963. A stereotaxic atlas of the brain of the squirrel monkey (*Saimiri sciureus*). Madison: University of Wisconsin Press.

Felleman DJ, Nelson RJ, Sur M, Kaas JH. 1983. Representations of the body surface in areas 3b and 1 of postcentral parietal cortex of Cebus monkeys. Brain Res 268:15–26.

Ferraina S, Bianchi L. 1994. Posterior parietal cortex: functional properties of neurons in area 5 during an instructed-delay reaching task within different parts of space. Exp Brain Res 99:175–178.

Fogassi L, Ferrari PF, Gesierich B, Rozzi S, Chersi F, Rizzolatti G. 2005. Parietal lobe: from action organization to intention understanding [see comment]. Science 308(5722):662–667.

Friedman D, Jones E. 1981. Thalamic input to areas 3a and 2 in monkeys. J Neurophysiol 45:59–85.

Friedman RM, Chen LM, Roe AW. 2004. Modality maps within primate somatosensory cortex. Proc Natl Acad Sci USA 101(34):12724–12729.

Gonzalo-Ruiz A, Leichnetz GR. 1990. Connections of the caudal cerebellar interpositus complex in a new world monkey (*Cebus apella*). Brain Res Bull 25(6):919–927.

Graziano MS, Taylor CS, Moore T. 2002. Complex movements evoked by microstimulation of precentral cortex. Neuron 34(5):841–851.

Grieve KL, Acuna C, Cudiero J. 2000. The primate pulvinar nuclei: vision and action. Trends Neurosci 23(1):35–39.

Huffman KJ, Krubitzer LA. 2001. Thalamo-cortical connections of areas 3a and M1 in marmoset monkeys. J Comp Neurol 435:291–310.

Ilinsky IA, Kultas-Ilinsky K. 2002. Motor thalamic circuits in primates with emphasis on the area targeted in treatment of movement disorders. Mov Disord 17(Suppl 3):S9–14.

Iriki A, Tanaka M, Obayashi S, Iwamura Y. 2001. Self-images in the video monitor coded by monkey intraparietal neurons. Neurosci Res 40:163–173.

Iwamura Y. 2000. Bilateral receptive field neurons and callosal connections in the somatosensory cortex. Phil Trans R Soc Lond B 355:267–273.

Iwamura Y, Iriki A, Tanaka M. 1994. Bilateral hand representation in the postcentral somatosensory cortex. Nature 369:554–556.

Iwamura Y, Tanaka M, Iriki A, Taoka M, Toda T. 2002. Processing of tactile and kinesthetic signals from bilateral sides of the body in the postcentral gyrus of awake monkeys. Behav Brain Res 135:185–190.

Jones EG. 1985. The thalamus. New York: Plenum Press.

Jones EG, Coulter JD, Hendry SHC. 1978. Intracortical connectivity of architectonic fields in the somatic sensory, motor and parietal cortex of monkeys. J Comp Neurol 181(2):291–348.

Jones EG, Powell TPS. 1969. Connexions of the somatic sensory cortex of the rhesus monkey. I. Ipsilateral cortical connections. Brain 92:477–502.

Jones EG, Wise SP, Coulter JC. 1979. Differential thalamic relationships of sensory-motor and parietal cortical fields in monkeys. J Comp Neurol 183:833–882.

Kaas JH, Nelson RJ, Sur M, Dykes RW, Merzenich MM. 1984. The somatotopic organization of the ventroposterior thalamus of the squirrel monkey, *Saimiri sciureus*. J Comp Neurol 226:111–140.

Kalaska JF. 1996. Parietal cortex area 5 and visuomotor behavior. Can J Physiol Pharmacol 74:483–498.

Kalaska JF, Scott SH, Cisek P, Sergio LE. 1997. Cortical control of reaching movements. Curr Opin Neurobiol 7:849–859.

Krubitzer L, Disbrow E. 2006. The evolution of parietal areas involved in hand use in primates. New York: Cambridge University Press.

Krubitzer LA, Kaas JH. 1990. The organization and connections of somatosensory cortex in marmosets. J Neurosci 10:952–974.

Krubitzer LA, Kaas JH. 1992. The somatosensory thalamus of monkeys: cortical connections and a redefinition of nuclei in marmosets. J Comp Neurol 319(1):123–140.

Kultas-Ilinsky K, Sivan-Loukianova E, Ilinsky IA. 2003. Reevaluation of the primary motor cortex connections with the thalamus in primates. J Comp Neurol 457(2):133–158.

Lacquaniti F, Guigon E, Bianchi L, Ferraina S, Caminiti R. 1995. Representing spatial information for limb movement: the role of area 5 in monkey. Cereb Cortex 5:391–409.

Lewis J, Van Essen D. 2000. Corticocortical connections of visual sensorimotor, multimodal processing areas in the parietal lobe of the macaque monkey. J Comp Neurol 428:112–137.

Lin CS, Merzenich MM, Sur M, Kaas JH. 1979. Connections of areas 3b and 1 of the parietal somatosensory strip with the ventroposterior nucleus in the owl monkey (*Aotus trivirgatus*). J Comp Neurol 185(2):355–371.

Loe PR, Whitsel BL, Dreyer DA, Metz CB. 1977. Body representation in ventrobasal thalamus of macaque: a single-unit analysis. J Neurophysiol 40(6):1339–1355.

Logothetis NK, Guggenberger H, Peled S, Pauls J. 1999. Functional imaging of the monkey brain [see comment]. Nat Neurosci 2(6):555–562.

Luppino G, Murata A, Govoni P, Matelli M. 1999. Largely segregated parietofrontal connections linking rostral intraparietal cortex (areas AIP and VIP) and the ventral premotor cortex (areas F5 and F4). Exp Brain Res 128(1–2):181–187.

Mayner L, Kaas J. 1986. Thalamic projections from electrophysiologically defined sites of body surface representations in areas 3b and 1 of somatosensory cortex of Cebus monkeys. Somatosens Res 4:13–29.

Merzenich MM, Kaas JH, Sur M, Lin C-S. 1978. Double representation of the body surface within cytoarchitectonic areas 3b and 1 in "SI" in the owl monkey (*Aotus trivirgatus*). J Comp Neurol 181:41–74.

Mountcastle VB, Lynch JC, Georgopoulos A, Sakata H, Acuña C. 1975. Posterior parietal association cortex of the monkey: command functions for operations within extrapersonal space. J Neurophysiol 38(4):871–908.

Murata A, Gallese V, Luppino G, Kaseda M, Sakata H. 2000. Selectivity for the shape, size, and orientation of objects for grasping in neurons of monkey parietal area AIP. J Neurophysiol 83(5):2580–2601.

Nelson RJ, Kaas JH. 1981. Connections of the ventroposterior nucleus of the thalamus with the body surface representations in cortical areas 3b and 1 of the cynomolgus macaque, *Macaca fascicularis*. J Comp Neurol 199:29–64.

Padberg J, Disbrow E, Krubitzer L. 2005. The organization and connections of anterior and posterior parietal cortex in titi monkeys: do New World monkeys have an area 2? Cerebral Cortex 2005;15(12):1938–1963.

Pandya DN, Seltzer B. 1982. Intrinsic connections and architectonics of posterior parietal cortex in the rhesus monkey. J Comp Neurol 204: 196–210.

Pearson JC, Haines DE. 1980. Somatosensory thalamus of a prosimian primate (*Galago senegalensis*). II. An HRP and Golgi study of the ventral posterolateral nucleus (VPL). J Comp Neurol 190(3):559–580.

Pearson RCA, Powell TPS. 1985. The projection of the primary somatic sensory cortex upon area 5 in the monkey. Brain Res Rev 9:89–107.

Pons TP, Kaas JH. 1985. Connections of area 2 of somatosensory cortex with the anterior pulvinar and subdivisions of the ventroposterior complex in macaque monkeys. J Comp Neurol 240:16–36.

Pons TP, Kaas JH. 1986. Corticocortical connections of area 2 of somatosensory cortex in macaque monkeys: a correlative anatomical and electrophysiological study. J Comp Neurol 248:313–335.

Rausell E, Jones EG. 1991. Histochemical and immunocytochemical compartments of the thalamic VPM nucleus in monkeys and their relationship to the representational map. J Neurosci 11:210–225.

Rizzolatti G, Fadiga L. 1998. Grasping objects and grasping action meanings: the dual role of monkey rostroventral premotor cortex (area F5). Novartis Found Symp 218:81–95; discussion 95–103.

Rizzolatti G, Fogassi L, Gallese V. 2001. Neurophysiological mechanisms underlying the understanding and imitation of action. Nat Rev Neurosci 2(9):661–670.

Rizzolatti G, Luppino G, Matelli M. 1998. The organization of the cortical motor system: new concepts. Electroencephalogr Clin Neurophysiol 106(4):283–296.

Sakata H, Taira M, Murata A, Mine S. 1995. Neural mechanisms of visual guidance of hand action in the parietal cortex of the monkey. Cereb Cortex 5:429–438.

Sakata H, Takaoka Y, Kawarasaki A, Shibutani H. 1973. Somatosensory properties of neurons in the superior parietal cortex (area 5) of the rhesus monkey. Brain Res 64:85–102.

Schmahmann JD, Pandya DN. 1990. Anatomical investigation of projections from thalamus to posterior parietal cortex in the rhesus monkey: a WGA-HRP and fluorescent tracer study. J Comp Neurol 295(2):299–326.

Shoham D, Grinvald A. 2001. The cortical representation of the hand in macaque and human area S-I: high resolution optical imaging. J Neurosci 21(17):6820–6835.

Stepniewska I, Fang PC, Kaas JH. 2005. Microstimulation reveals specialized subregions for different complex movements in posterior parietal cortex of prosimian galagos. Proc Natl Acad Sci USA 102(13):4878–4883.

Stepniewska I, Preuss TM, Kaas JH. 1994a. Architectonic subdivisions of the motor thalamus of owl monkeys: Nissl, acetylcholinesterase, and cytochrome oxidase patterns. J Comp Neurol 349(4):536–557.

Stepniewska I, Preuss TM, Kaas JH. 1994b. Thalamic connections of the primary motor cortex (M1) of owl monkeys [erratum appears in J Comp Neurol 1995;353(1):160]. J Comp Neurol 349(4):558–582.

Sur M, Nelson RJ, Kaas JH. 1982. Representations of the body surface in cortical areas 3b and 1 of squirrel monkeys: comparisons with other primates. J Comp Neurol 211:177–192.

Tanne-Gariepy J, Rouiller EM, Boussaoud D. 2002. Parietal inputs to dorsal versus ventral premotor areas in the macaque monkey: evidence for largely segregated visuomotor pathways. Exp Brain Res 145(1):91–103.

Taoka M, Toda T, Iriki A, Tanaka M, Iwamura Y. 2000. Bilateral receptive field neurons in the hindlimb region of the postcentral somatosensory cortex in awake macaque monkeys. Exp Brain Res 134:139–146.

Veenman C, Reiner A, Honig M. 1992. Biotinylated dextran amine as an anterograde tracer for single- and double-label studies. J Neurosci Methods 41:239–254.

Vitek JL, Ashe J, DeLong MR, Alexander GE. 1994. Physiologic properties and somatotopic organization of the primate motor thalamus. J Neurophysiol 71(4):1498–1513.

Vitek JL, Ashe J, DeLong MR, Kaneoke Y. 1996. Microstimulation of primate motor thalamus: somatotopic organization and differential distribution of evoked motor responses among subnuclei [erratum appears in J Neurophysiol 1997;77(6):2857]. J Neurophysiol 75(6):2486–2495.

Wise SP, Boussaoud D, Johnson PB, Caminiti R. 1997. Premotor and parietal cortex: corticocortical connectivity and combinatorial computations. Annu Rev Neurosci 20:25–42.

Yeterian EH, Pandya DN. 1985. Corticothalamic connections of the posterior parietal cortex in the rhesus monkey. J Comp Neurol 237:408–426.